Caving 2010 — Y. Potvin (ed)

doi:10.36487/ACG_rep/1002_9_Elmo

An integrated finite/discrete element method – discrete fracture network synthetic rock mass approach for the modelling of surface subsidence associated with panel cave mining at the Cadia East underground project

D. Elmo *Golder Associates Ltd., Canada*

S. Rogers *Golder Associates Ltd., Canada*

R. Beddoes *Golder Associates Ltd., Canada*

A. Catalan *Newcrest Mining Limited, Australia*

Abstract

The ability to predict surface subsidence associated with mass mining methods is important for both environmental impact and operational hazard assessments, however, the fundamental understanding of the complex rock mass response in block/panel cave mining settings remains limited. In this context, the use of numerical modelling provides an opportunity to investigate the factors governing caving mechanisms and to develop improved methodologies for the prediction of associated surface subsidence. In this paper the authors adopt an integrated numerical approach based on the analysis of the mechanical behaviour of discrete systems. This includes both more realistic representation of fracture systems and the modelling of rock mass behaviour as a combination of failure through intact rock material and displacement/rotation along predefined discontinuity planes.

The focus of this paper is the numerical analysis of the factors controlling caving and associated subsidence, with emphasis on the potential impact of major geological structures and draw control. The numerical results clearly illustrate the importance of jointing and faulting conditions on subsidence development mechanisms and further emphasise the governing role of geological structure in defining the degree of surface subsidence asymmetry. The integrated modelling approach is shown to fully capture the complex rock mass response to caving associated with multi lift extraction and the modelled results are in agreement with analytical methods for simulation of gravity flow.

It is argued that the predictive character of the integrated finite/discrete element method (FEM/DEM) - discrete fracture network (DFN) approach is beneficial in providing useful information particularly at the earlier stages of block/panel cave development. This allows the comparison of various mining scenarios, helping the mining engineers and mine management to select the best path forward.

1 Introduction

Mass mining (block and panel cave mining) is one of the most cost effective underground mining techniques. High efficiency and low production costs coupled with a growing demand on natural resources have led to the increasing importance of this mining method in the mining industry. A typical cave mine layout consists of two mining levels (a production and an undercut level respectively) placed within the ore column. Ore is mined sequentially in large sections over areas of several thousands of square metres. Caving is initiated by blasting an extensive horizontal panel (undercut) under the mined block. Stress redistribution and gravity combine to trigger progressive fracturing and caving of the ore into the undercut. As caving of the ore is initiated, the undercut is connected with the production level by blasting ore passages, called drawbells. As the fragmented ore is extracted, the ore above continues to break and cave by gravity. As a result, caving extends progressively upwards, potentially causing significant deformations above the undercut and in the adjacent areas. In this context, the ability to predict surface subsidence associated with block and panel cave mining is becoming increasingly important for mine planning and operational hazard assessment. Owing to

problems of scale and lack of access, the fundamental understanding of the complex rock mass response leading to subsidence remains limited, as are current subsidence prediction capabilities.

Numerical methods overcome some of the limits of the empirical methods and provide an opportunity to increase our fundamental understanding of the factors governing caving induced subsidence. This paper presents selected results of a FEM/DEM-DFN numerical modelling study of surface subsidence associated with panel cave mining at the Cadia East underground project, focusing on the role of rock mass fabric and faults on surface subsidence development.

2 An integrated FEM/DEM-DFN approach to the numerical analysis of caving induced surface subsidence

2.1 Geomechanical modelling

Cave development and surface subsidence are the products of complex rock mass response, which comprises massive, brittle fracture driven failure of the rock mass, both in tension and compression, along existing discontinuities and through intact rock bridges. Additionally, cave development and block caving subsidence almost invariably involves complex kinematic mechanisms.

To simulate these complex mechanisms using numerical modelling, a numerical analysis has to incorporate a realistic representation of the mechanical behaviour of discrete fracture systems. By definition, the utilisation of a continuum approach to model a process that is ultimately discontinuous has intrinsic limitations and cannot capture all the subtleties of brittle failure. From a modelling perspective, brittle fracturing corresponds to a transition from a continuum to a discontinuous state. To satisfy this condition, the current modelling employs a state-of-the-art hybrid FEM/DEM technique, incorporating fracture mechanics principles in combination with the finite/discrete element method to simulate caving processes in a more realistic manner than one approach alone. There are significant advantages in employing a combined FEM/DEM solution strategy to model discrete/discontinuous systems, including:

- A better description of the physical processes involved, accounting for diverse geometric shapes and effective handling of large numbers of contact entities with specific interaction laws.
- The implementation of specific fracture criteria and propagation mechanisms allows the simulation of the progressive fracture process within both the finite and discrete elements.
- Accounting for the full representation of the anisotropic and inhomogeneous effects of natural jointing.

The ELFEN code (Rockfield, 2009) used in the current study is a multipurpose FEM/DEM software package that utilises a variety of constitutive criteria and is capable of both implicit and explicit analyses in two and three-dimensions (2D/3D). It has the capability to simulate continuum materials, jointed media and particle flow behaviour. The ELFEN computational methodology has been extensively tested and validated fully against controlled laboratory tests by Yu (1999) and Klerck (2000). Among others, research by Cai and Kaiser (2004), Stead et al. (2004), Elmo (2006), Stefanizzi (2007) and Elmo and Stead (2009) has demonstrated the capabilities of the code in the analysis of various rock mechanics problems involving brittle failure, including analysis of Brazilian, unconfined compressive strength (UCS) and direct shear laboratory tests, analysis of slope failures, and underground pillar stability. Recent work by Yan (2008) has illustrated that ELFEN simulations of laboratory-scale step-path failure under axial compression are in good agreement with actual physical tests and correlate well with modelling results obtained by other codes. There are several examples in the literature of block cave modelling in ELFEN, including Elmo et al. (2007, 2008), Pine et al. (2007), Vyazmensky (2008) and Vyazmensky et al. (2009a, 2009b).

Where large scale geometries are modelled in 2D and 3D, there is an inherent problem in the need to use large elements dimensions due to computing limitations. Furthermore, extrapolation of brittle rock fracture mechanics processes from laboratory scales (less than 1 mm mesh size) to intact rock fracture through/between metre scale blocks/particles requires careful engineering judgement. Stead et al. (2007) has discussed the relationship between model scale, mesh size and number of elements used in current practice for 2D discrete numerical analysis of rock engineering problems. Even for simple 2D brittle fracture models,

modelling of large engineering structures requires a relatively large element size (greater than 2 m). When these models are contemplated in 3D, the magnitude of the computing problem is immediately apparent and arguably challenging if fracturing is to be modelled at a realistic scale.

Because model uncertainty increases with the scale of the problem under consideration, a tiered approached toward scale of modelling has to be considered that is strongly related to both structural observations and rock mass quality. A brittle fracture model requires simplification in order to make the problem tractable and care is required not to 'smooth-out' critical structural features. Consideration is given to model design to highlight critical features so that the mesh may be refined appropriately. Constitutive criteria incorporating fracture are used in specific locations as opposed to the whole model geometry to provide potential savings in computer memory.

2.2 DFN modelling

Caving induced subsidence potentially involves complex kinematic mechanisms. To simulate these mechanisms accurately using numerical modelling, the current modelling approach incorporates a representation of the mechanical behaviour of discrete fracture systems. This involves the simulation and representation of fracture networks as a collective system of fracture sets. In this context the DFN approach represents an ideal numerical tool for the synthesis of realistic fracture network models from available field data. The DFN approach has the capability of defining geological models which include large (deterministic) structures as well as stochastically generated fracture systems. The proprietary code FracMan (Dershowitz et al., 1998; Golder Associates, 2009) is the platform used in the current paper for data synthesis. Each fracture set within a single structural domain is characterised in FracMan using statistical distributions to describe variables such as the orientation, persistence and spatial location of the fractures.

The FracMan DFN model of Cadia East (Rogers et al., 2010) is used to derive 2D fracture traces which are subsequently embedded in the 2D ELFEN models to maximise the quality of representation of the geometry of the existing rock jointing and to account fully for anisotropic rock mass response. The use of a fully 3D DFN model as the source of fracture traces for 2D geomechanics analysis requires careful engineering judgment to avoid altering the mode and characteristics of potential kinematic instability and the introduction of fictional rock bridges. A filtering process is applied to the initial 3D DFN model prior to use in a 2D analysis, which includes, for instance, synthesising only fracture sets whose dip direction is parallel to subparallel to the assumed 2D section. In the current models, a filter of ±20 degrees relative to the section azimuth is applied.

3 The Cadia East underground project

Fully owned by leading Australian gold producer Newcrest Mining Ltd., and located within the Cadia Valley Province in central New South Wales (Australia), the Cadia East underground project is planned to become the deepest panel cave in the world and Australia's largest underground mine. Panel caving has been selected as the preferred mining method on the basis of most favourable technical and economic outcomes for development of the orebody, which consists of a porphyry zone of gold-copper mineralisation adjacent to the eastern edge of the Cadia Hill orebody and extending to up to 2.5 km east.

Figure 1 shows cross sections through the Cadia East orebody (Catalan et al., 2008); with indication of the different geological domains and location of the planned undercut levels (Lift-0 and Lift-1 respectively). This paper specifically presents modelling results describing mine plan scenarios discussed as part of the prefeasibility study (PFS).

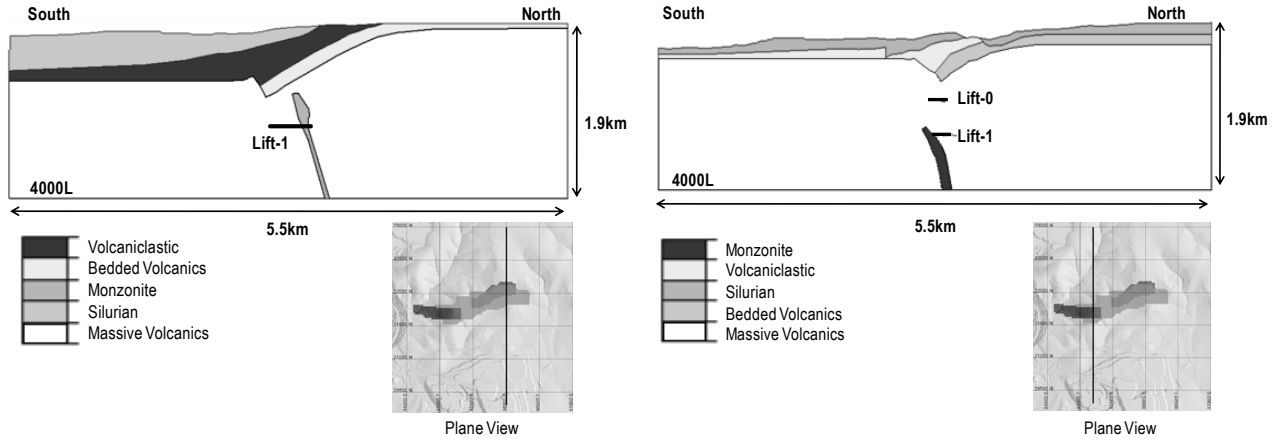

Figure 1 Cross section through the Cadia East orebody: (left) Model 15100E; and (right) Model 16000E

4 Modelling methodology

4.1 Rock mass properties

The rock mass can be represented in ELFEN using a variety of constitutive criteria including a Rankine rotating crack material model, in which fracturing is controlled by tensile strength and fracture energy parameters. For tension/compression stress states, the Rankine model is complemented with a Mohr–Coulomb criterion in which the softening response is coupled to the tensile model. For discrete fracturing analysis, a discrete crack is introduced when the maximum principal stress exceeds the tensile yield strength of the material.

As part of the PFS for Cadia East, the necessary material parameters for numerical analysis have been derived according to empirical relationships based on rock mass classification systems. The rock mass classification system used in the current analysis is the Geological Strength Index (GSI) (Hoek et al., 1995) and specific GSI data for each geological domain at Cadia East were provided by Newcrest Mining Ltd. (Catalan et al., 2008). Rock mass internal cohesion, internal friction angle and deformation modulus were estimated using the coupled GSI-RocLab approach (Hoek et al., 2002), assuming specific values for the parameter m_i and a σ_{3max} value of 10 MPa in RocLab. At this stage of the analysis, the values of Young's Modulus for the intact rock were assumed based on typical values for sedimentary and volcanic rock types. The rock mass tensile strength (σ_{tm}) was assumed as 10% of the theoretical value calculated using the Mohr–Coulomb criterion.

Table 1 Rock mass material properties used in the ELFEN Models

	σ_{ci} MPa	GSI	m_i	E_i MPa	c MPa	φ Deg.	E_m MPa	σ_{tm} MPa
Silurian sediments	120	45	12	30,000	2.9	39.7	6,709	0.3
Volcaniclastic	170	59	12	50,000	4.4	46.6	24,864	0.3
Volcanic bedded	133	61	12	50,000	4.1	45.2	27,135	0.3
Volcaniclastic massive	170	62	15	50,000	4.8	49.3	28,266	0.4
Monzonite	145	62	18	50,000	4.6	49.6	28,266	0.3

4.2 Simulation of draw sequence

Cave propagation is induced by the removal of fragmented ore on the production level. To simulate this process within the current finite-discrete approach, a specific algorithm is used that removes all the meshed elements whose centroids are located within a specified region, and in this case corresponding to the undercut level. Equivalent boundary forces on the floor and walls of the undercut are used to simulate the support that the bulked material effectively provides to the surrounding rock mass. An iterative process is used such that the removal of elements is repeated continuously at a given numerical time step in order to return the specified draw rate, and the model is calibrated to yield a draw rate of approximately 100 mm/day.

Because of the 2D nature of the modelling, a pseudo-volume of removed ore material has to be defined to constrain the simulated draw rate. The procedure adopted in the current study involve the use of the mine plans provided, specifically height of draw (HOD) and tonnes per drawpoint which define a pseudo target volume (volume · year^{-1}), herein expressed as 'mined block area'. Draw zones are defined by grouping together all the drawpoints within ±15 m of the section azimuth and for each zone an average HOD is calculated. The mined block area is subsequently calculated by multiplying the average HOD by the width of the draw zone and assuming unit length in the out of plane direction. Figures 2 and 3 show the mined block area at various stages of the mine life for models 15100E and 16000E respectively.

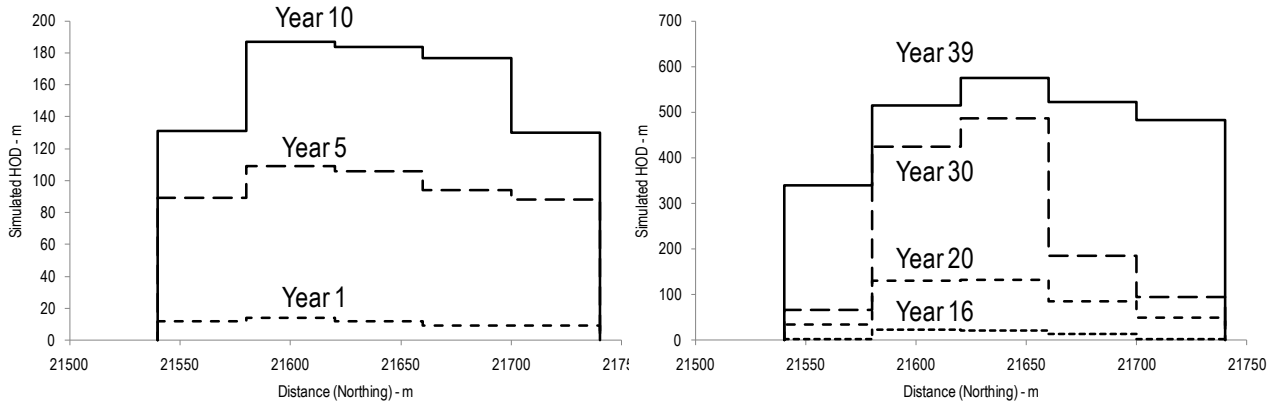

Figure 2 Mined block area at varying stages of the simulation for model 15100E, Lift-0 (left); and Lift-1 (right)

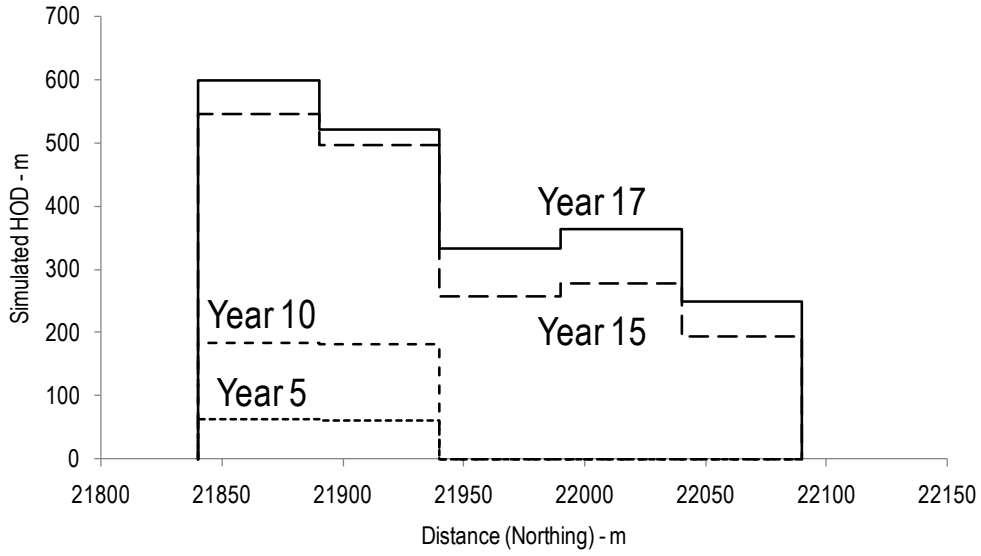

Figure 3 Mined block area at varying stages of the simulation for model 16000E

5 2D modelling results – influence of rock fabric and geological structures

Mining experience suggests that, among other contributing factors, rock fabric and geological faults represent important factors controlling cave development and surface subsidence. Vyazmensky et al. (2009b) have argued that qualitative rather than quantitative description of the influence of geological structures on the observed subsidence is provided in published material. The modelling results presented in the following sections attempt to provide a quantitative framework to this issue with specific reference to the mine plan scenarios as part of the PFS of Cadia East panel cave project.

5.1 Model for 2D section 16000E

The simulated draw rate varies between 90–110 mm/day. The comparison between the target mined block area and the simulated results is shown in Figure 4. The good agreement between simulated results and planned production indicates the degree of effectiveness of the algorithm used to simulate ore removal in ELFEN 2D. Modelled advance to draw rate ratio is 2:2.2.

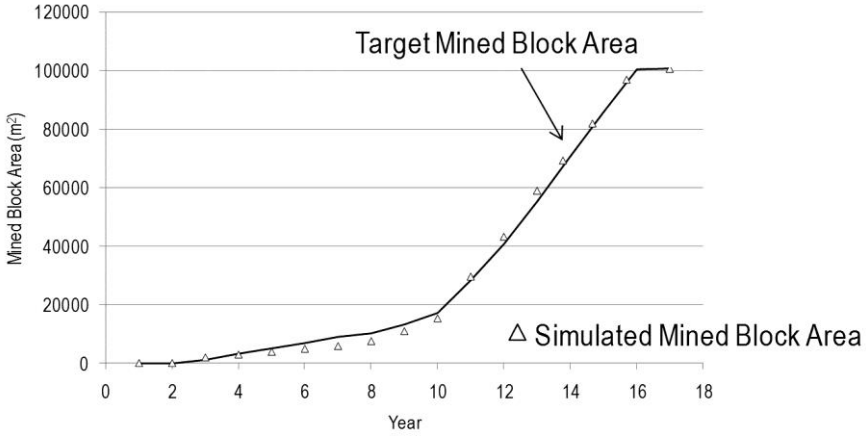

Figure 4 16000E model, comparison between target mined block area and simulated results

A different modelled response to caving is observed in the model for the Monzonite domain compared to the Massive Volcanics rock mass (see Figure 5), though the two domains have similar rock mass properties. In the current model, a 600 m high × 300 m wide area above the extraction zone is used with a mesh discretisation of 3 m to represent the orebody, whilst the size of the mesh is increased to 6 m for the outside rock mass. As the undercut is excavated and the cave front extends laterally within the Massive Volcanics domain, the contact between Massive Volcanics and Monzonite acts as a discontinuity. Once the cave front reaches the contact, then fracturing cannot extends across, leaving relatively large unfractured portions of Monzonite within the de-stressed cave zone. As a result, these larger blocks move down the cave zone without undergoing much secondary breakage. No hang-ups can be simulated at the extraction level since the simulated draw is designed to gradually 'break' the rock passing through the extraction level (i.e. ideal draw scenario is assumed in the model). The use of a different mesh size to represent the ore block indirectly shows potential dilution effects occurring at a later stage of the mine life (Year 14 and onwards), though a quantitative analysis of dilution has not been attempted at this stage.

The results for the 16000E model indicate that jointing and major geological faults will have a large impact on cave shape. The presence of the subvertical joint set results in a preferred cave propagation direction, though in the current models the effects of the pre-existing joint pattern are minimal compared to the influence of the included geological faults. As shown in Figure 7, up to Year 9.6 the cave appears to be fully contained within two major geological structures. The [-1 m, -0.2 m] range of vertical displacement highlights the asymmetric caving induced deformations, characterised in terms of the angle between the direction of max deformation and vertical axis. The cross-over occurs when the cave front reaches a point along Fault A that corresponds to the fault's dip angle varying from steep to shallow. The overall cross-over mechanism is clearly influenced by the presence of a north dipping fault (C) normal to the cave front. As the caved zone is not longer bounded by the two main faults (A and B), its advance becomes more controlled by the subvertical joint set.

The modelling results for 16000E model indicate a rapid increase of the subsidence rate after Year 12, the cave propagating through the Silurian sediments primarily through progressive flexural failure of largely unfractured blocks. Maximum simulated subsidence depth for Model 16000 is 30 m, though consolidation of the caved rock may result in an increased width and depth of the simulated subsidence crater.

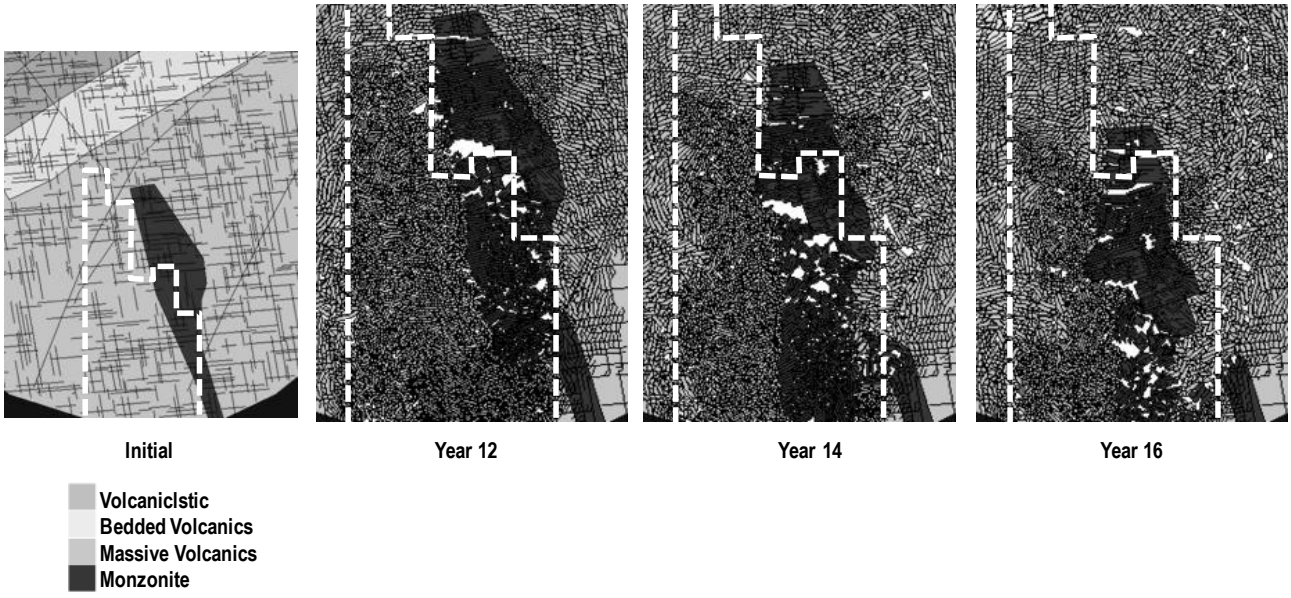

Figure 5 Model 16000E, different simulated response to caving observed for the Monzonite domain compared to the Massive Volcanics rock mass. The dashed line indicates the shape of the mined block area at Year 17 as shown in Figure 3

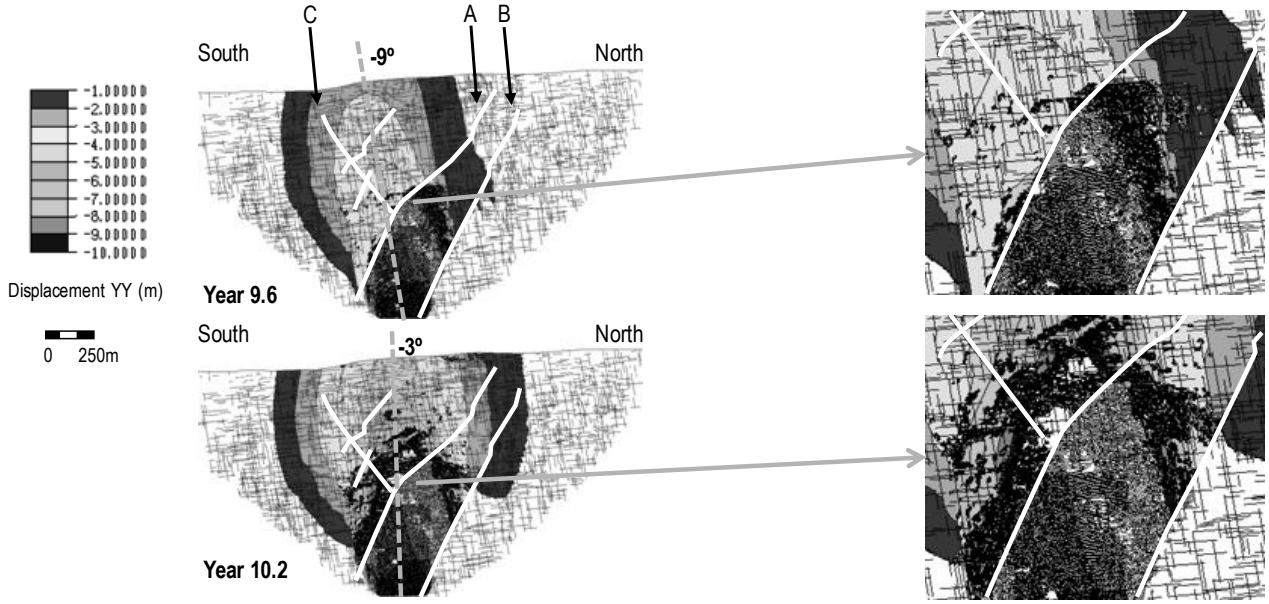

Figure 6 Model 16000E, simulated impact of major geological faults (white lines) and jointing on cave propagation, showing the cross-over mechanism

5.2 Model for 2D section 15100E

The main objective of the current model is to provide indications with respect to cave advance, surface subsidence and cave interaction between two sequential lifts. The simulated draw rate varies between 60–110 mm/day. The comparison between the planned mined block area and the simulated results, Figure 7,

indicates an overall good agreement. Arch formation within the caving rock mass explains the relatively smaller differences observed between the two curves. The simulated draw rate increases as these arching effects are no longer sustained.

Figure 8 shows the extent of the caved zone between Year 5 and Year 15. The modelled ratio between cave advance to draw rate is approximately 300 mm/day (advance) to 80 mm/day (draw). The occurrence of a subhorizontal joint set is shown in the literature to favour cave propagation, accordingly the model indicates that the mobilised cave zone will advance vertically at a relatively rapid rate. In the current model, the failure of the rock bridges between the subvertical set also contributes to control the direction of cave propagation, the resulting structural features providing low shear strength surfaces for the rock mass to slide under the influence of gravity. The presence of major geological structures (faults) is shown to influence cave propagation as well, the Lift-0 cave breakthrough being controlled near surface by a south dipping fault. Limited subsidence is shown by the end of Year 15, prior to the initiation of the Lift-1 cave, and the estimated subside rate is on average 110 mm/year, estimated for the period from Year 1 to Year 15.

The excavation of the undercut zone for Lift-1 is initiated at Year 15. The extent of the caved zone between Year 16 and Year 28 is shown in Figure 9. Cave propagation is shown to be strongly influenced by the predefined combined joints/faults pattern. Cave development is clearly asymmetric in a northerly direction, with relatively large induced horizontal deformations resulting in the formation of near surface tensile fracturing.

The interaction between the two caves is controlled by the stress redistribution associated with the presence of the Lift-0 cave as shown in Figure 10. The crown pillar between Lift-1 and the overlying Lift-0 initially becomes increasingly stressed, favouring clamping of the subvertical joints and failure through delamination along the subhorizontal set. As the caved zone from Lift-1 migrates upwards and connects with the abutments of the Lift-0 extraction level, fractured zones are formed that result in the remnant crown pillar to undergo almost exclusively flexural failure, with large portions of unfractured rock mass becoming mobilised within the de-stressed cave zone.

Because of the lower shear strength of the fractured zones connecting the Lift-1 cave front with the abutments of the Lift-0 extraction level, the simulated failure of the crown pillar is rapid and consequently the caved material left behind in Lift-0 is suddenly mobilised into the underlying Lift-1 cave, Figure 11. By Year 29 the pre-existing faults are almost fully contained within the mobilised caved zone, accordingly their influence on cave propagation is not longer felt. The cave shape at Year 29 is almost symmetrical as indicated by the values of the cave angles.

For section 15100E localised arching, possibly associated with the consolidation of the caved material, is observed in the models between Year 10 and Year 15. These arching effects are no longer sustained as the cave zone from Lift-1 propagates upwards, culminating in the rapid increase of the simulated maximum subsidence depth, from 2 m depth at Year 28 to approximately 57 m depth at Year 36.

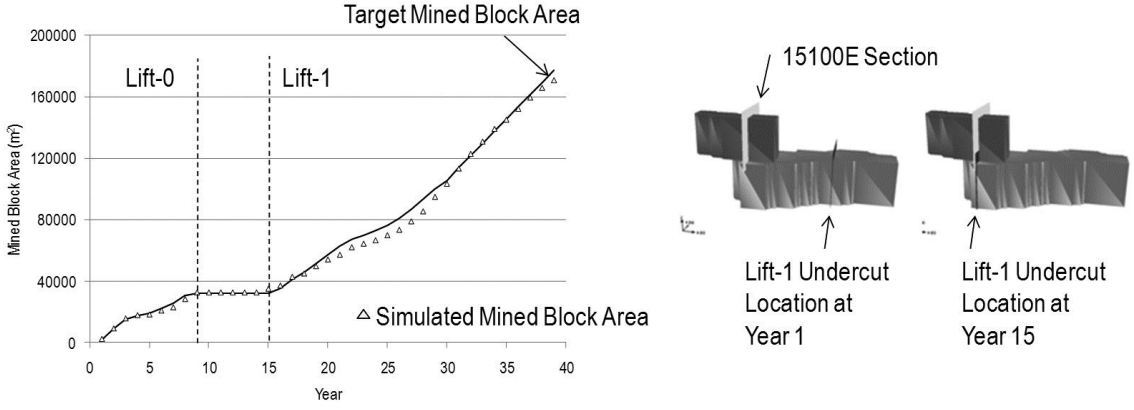

Figure 7 Model 15100, comparison between target mined block area and the simulated results. Note that caving of Lift-0 precedes caving of Lift-1, with a hiatus during which the undercut of Lift-1 is advanced to the 15100E section

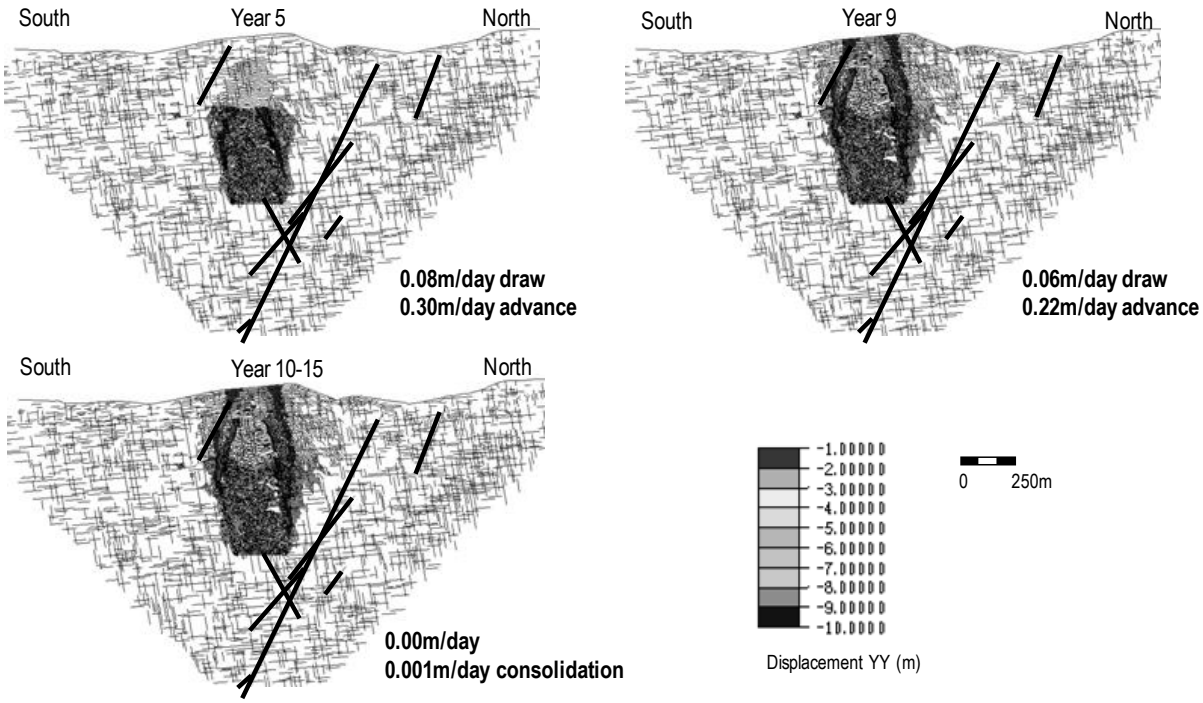

Figure 8 **Model 15100E, extent of the caved zone (indicated by the -1 m vertical displacement) between Year 5 and Year 15. The simulated advance and draw rates are also indicated. Thick black lines indicate major geological structures**

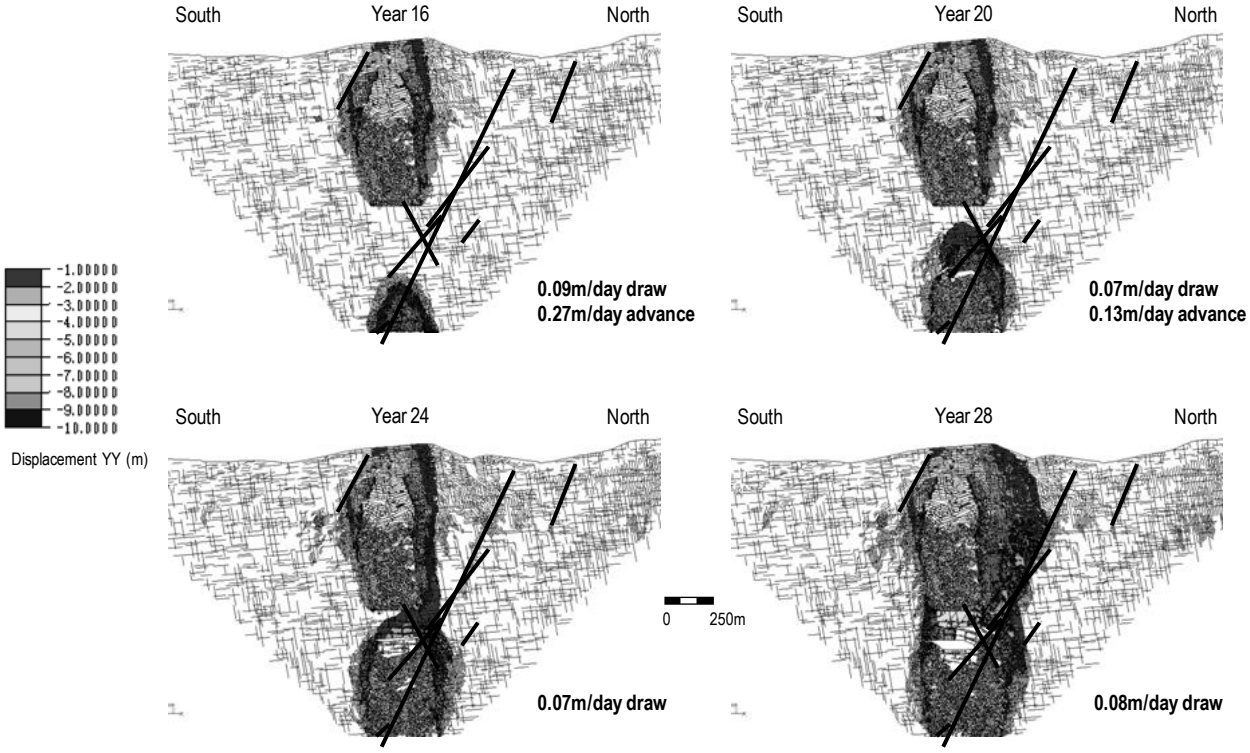

Figure 9 **Model 15100E, extent of the caved zone (indicated by the -1 m vertical displacement) between Year 16 and Year 28. The simulated advance and draw rates are also indicated. Thick black lines represent pre-existing major faults**

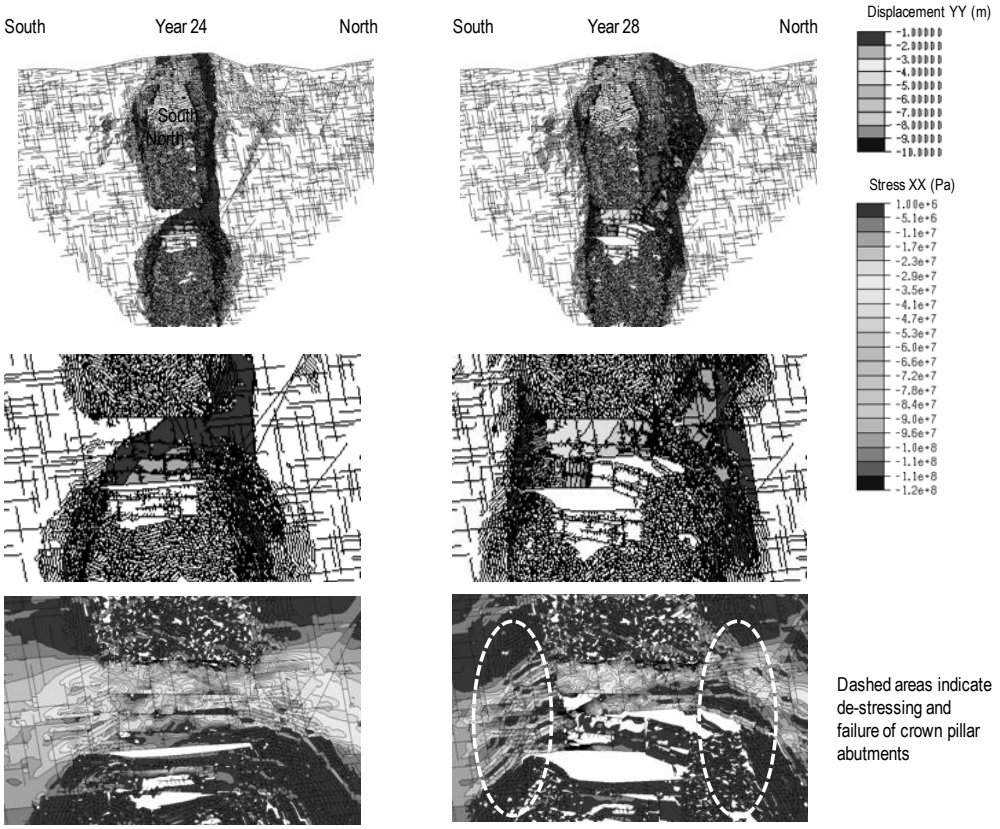

Figure 10 Model 15100E, simulated interaction between Lift-0 and Lift-1

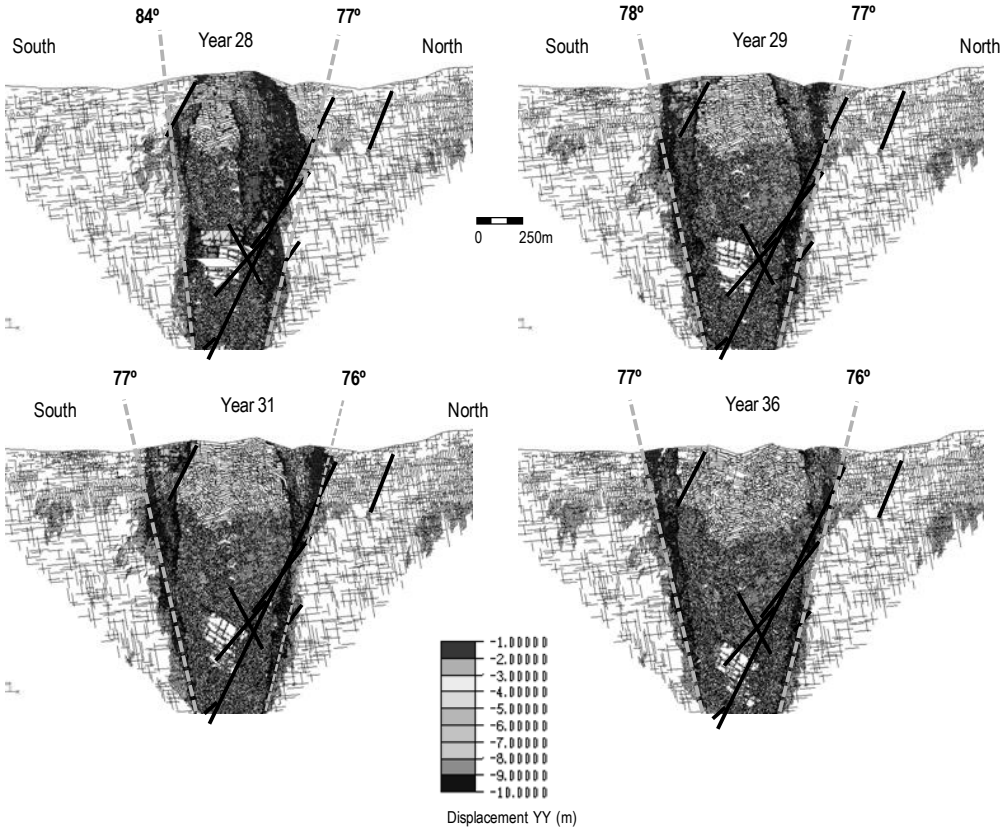

Figure 11 Model 15100E, extent of caved zones and estimated angles of break at Year 28, Year 29, Year 31 and Year 36 respectively and subsidence rate (m/year)

6 Comparison of ELFEN 2D results to analytical methods for simulation of gravity flow

The prefeasibility character of the current modelling is such that no direct calibration (using monitoring data) is possible. As an indirect form of validation, it was decided to compare the simulated results with analytical methods of cave analysis. The comparison was performed using the 16000E model as reference. The volume of rock that fails into any given cave will be controlled by the cave dimensions and the bulking factor of the overlying rock mass. This volume of rock can be defined by the draw envelope, or draw ellipsoid, and the volume of rock in which movement takes place is defined by the limit envelope, or limit ellipsoid (Kvapil, 1992). The volume of the ellipsoid, assuming the equatorial radii (along the x and y axes) *a* and *b* are equal, and *c* represents the polar radius (along the z-axis), is given by:

$$V = \frac{4}{3}\pi a^2 c \tag{1}$$

Assuming a is the width of the simulated undercut zone and c is the HOD, the equation above can be used to calculate the volume of failed rock within the ellipsoid, by dividing the volume of the ellipsoid by a given bulking factor (1.4 is used in the current analysis). This provides the volume of failed rock or draw ellipsoid, and its height can be estimated by solving the equation above for c. In the literature the volume of the limit ellipsoid is reported as about 15 times greater than the volume of the draw ellipsoid. Accordingly the height of the limit ellipsoid could be approximated as 2.5 times the height of the ellipsoid of draw. The shape of a given ellipsoid of motion can be described by its eccentricity, and eccentricity values in the range of 0.92–0.96 are reported in the literature as being most common. By repeating the analysis for a HOD of 25, 144, 260 and 400 m, the estimated vertical extent of failure above the cave (height of limit ellipsoid) is plotted against the corresponding HOD. The results of the analytical solution are compared with the simulated results for the 16000E model, assuming a given ellipsoid shape to match the simulated extend of the caved zone. Overall, there is a good agreement between modelled and theoretical values and indicated by Figure 11. The apparent difference between theoretical and simulated results is explained by considering the degree of asymmetry of the modelled cave zone. By Year 16, an exact limit ellipsoid cannot be fit to the modelled results, and two approximated limit ellipsoid (A and B) are therefore indicated. Estimated eccentric values are also calculated and indicated in Figure 12.

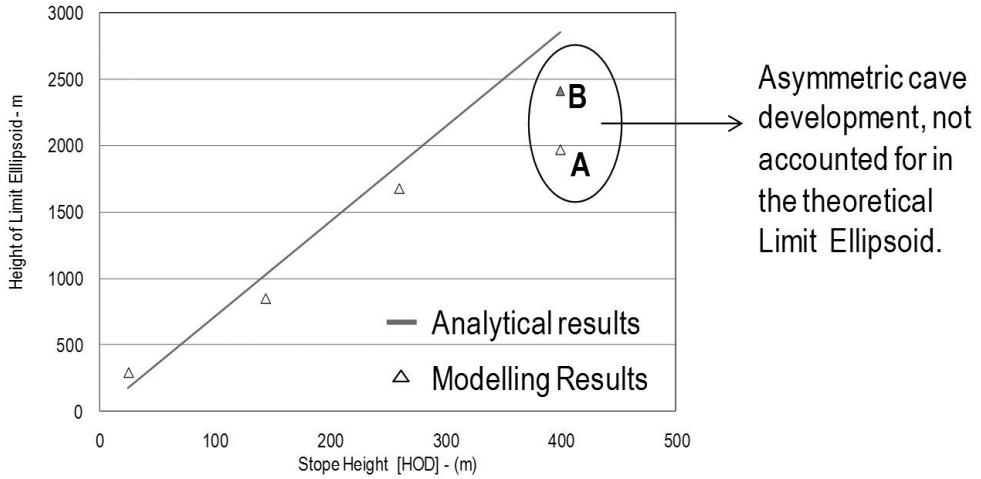

Figure 12 Comparison between the limit ellipsoid estimated according to the theory (assuming an undercut width of 250 m) and simulated results for the 16000E model

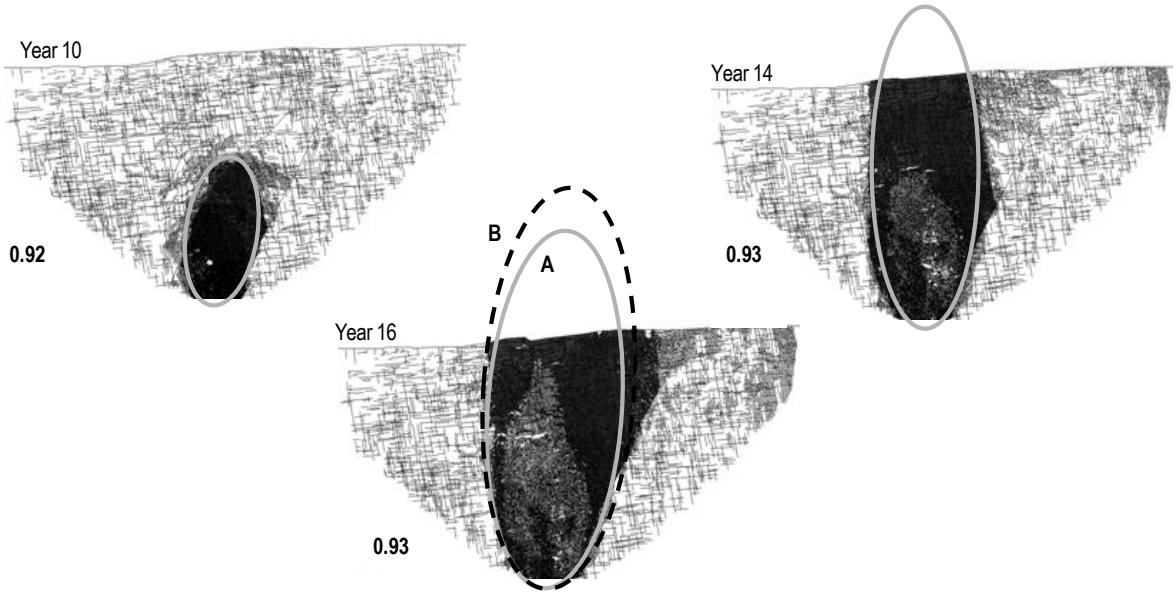

Figure 13 Model 16000E, estimated limit ellipsoid at different stages of the mine life. Eccentricity values are also indicated. A and B refer to results shown in Figure 11

7 Discussion

To the authors' knowledge the current study represent the first application of a discrete fracture modelling approach to an industrial scale project to characterise cave development and surface subsidence. It is worth noticing that in the current study no assumptions have been made regarding the cave development, which in the model is purely a function of the assumed rock mass properties, undercut advance and material extraction. The results have shown that a discrete fracture modelling approach can effectively capture important cave mechanisms, including preferential rock fragmentation within the ore column and the potential controlling role of rock fabric and geological structures on cave development and surface subsidence.

Whereas 3D analysis of geomechanical problems is ultimately desired, 3D simulation of caving mechanisms has to date almost exclusively involved continuum modelling. It is argued that this choice is driven by the higher computational efficiency of continuum codes for large scale modelling. However, continuum codes are unable to simulate explicitly caving mechanisms (e.g. brittle fracture and kinematic driven failure) and therefore may not be applicable in all cases. As discussed by Stead et al. (2007), the application of discontinuum codes for cave analysis poses intense computational challenges. In the authors' opinion the discrete modelling approach presented in this paper provides a valuable tool in the rock engineer's geotechnical modelling toolbox. As the requisite computing power becomes available and codes are adapted to make use of 64 bit architectures and parallel processing facilities, existing hybrid finite-discrete element techniques could be adopted for large scale 3D modelling of mining problems.

Acknowledgements

The authors would like to acknowledge Newcrest Mining Ltd, who kindly gave permission to publish the modelling results presented in this paper.

References

Cai, M. and Kaiser, P.K. (2004) Numerical simulation of the Brazilian test and the tensile strength of anisotropic rocks and rocks with pre-existing cracks, in Proceedings SINOROCK International Symposium on Rock Mechanics: Rock characterization, modelling and engineering design methods, 18–21 May, Three Gorges Project site, China, Paper 2B–03.

Catalan, A., Suarez, C., Barrera, V. and Qudraturrahman, I. (2008) Cadia East underground project Pre-Feasibility Study, Geotechnical Report, Newcrest Mining Limited Internal Document.

Dershowitz, W., Lee, G., Geier, J. and LaPointe, P.R. (1998) FracMan: Interactive discrete feature data analysis, geometric modelling and exploration simulation, User Documentation, Golder Associates Inc., Seattle, Washington.

Elmo, D., Vyazmensky, A., Stead, D. and Rance, J.R. (2007) A hybrid FEM/DEM approach to model the interaction between open pit and Numerical Analysis of Block Caving-Induced Instability in Large Open Pit Slopes, in Proceedings 1st Canada-U.S. Rock Mechanics Symposium, Vancouver, Canada.

Elmo, D. (2006) Evaluation of a hybrid FEM/DEM approach for determination of rock mass strength using a combination of discontinuity mapping and fracture mechanics modelling, with particular emphasis on modelling of jointed pillars, PhD Thesis, Camborne School of Mines, University of Exeter, UK.

Elmo, D. and Stead, D. (2009) An integrated numerical modelling – discrete fracture network approach applied to the characterisation of rock mass strength of naturally fractured pillars, Rock Mechanics and Rock Engineering, DOI 10.1007/s00603-009-0027-3.

Elmo, D., Vyazmensky, A., Stead, D. and Rance, J. (2008) Numerical analysis of pit wall deformation induced by block-caving mining: A combined FEM/DEM–DFN synthetic rock mass approach, in Proceedings 5th Conference and Exhibition on Mass Mining, Luleå, Sweden, June 2008, 10 p.

Golder Associates (2009) FracMan 7.20, FracMan Technology Group, Golder Associates Inc., Seattle, Washington.

Hoek, E.T., Kaiser, P.K. and Bawden, W.F. (1995) Support of underground excavations in hard rock, A.A. Balkema Rotterdam, 215 p.

Hoek, H.Y., Carranza Torres, C. and Corkum, B. (2002) Hoek–Brown Failure Criterion – 2002 edition, RocLab user's manual.

Klerck, P.A. (2000) The finite element modelling of discrete fracture in quasi-brittle materials, PhD thesis, University of Swansea, UK.

Kvapil, R. (1992) Sublevel caving, SME Mining Engineering Handbook, 2nd Edition, H.L. Hartman (ed), SME, Littleton, Colorado, pp. 1789–1814.

Pine, R.J., Owen, D.R.J., Coggan, J.S. and Rance, J.M. (2007) A new discrete modelling approach for rock masses, Geotechnique, Vol. 57, No. 9, pp. 757–766.

Rockfield Software (2009) ELFEN Version 4.3.3, Swansea, UK.

Rogers, S., Elmo, D.,Webb, G. and Catalan, A. (2010) A discrete fracture network based approach to defining in situ, primary and secondary fragmentation distributions for the Cadia East panel cave project, in Proceedings 2nd International Symposium on Block and Sublevel Caving (Caving 2010), Y. Potvin (ed), 20–22 April 2010, Perth, Australia, Australian Centre for Geomechanics, Perth, pp.425–440.

Stead, D., Elmo, D., Yan, M. and Coggan, J. (2007) Modelling brittle fracture in rock slopes: experience gained and lessons learned, in Proceedings International Symposium on Rock Slope Stability in Open Pit Mining and Civil Engineering, September, Perth, Australia.

Stead, D., Coggan, J.S. and Eberhardt, E. (2004) Realistic simulation of rock slope failure mechanisms: the need to incorporate principles of fracture mechanics, in Proceedings SINOROCK International Symposium on Rock Mechanics: Rock characterization, modelling and engineering design methods, 18–21 May, Three Gorges Project site, China, Paper 2B–17.

Stefanizzi, S. (2007) Numerical modelling of strain-driven fractures around tunnels in layered materials, PhD Thesis, University of Turin, Italy.

Vyazmensky, A. (2008) Numerical modelling of surface subsidence associated with block cave mining using a finite element/discrete element approach, PhD thesis, Simon Fraser University, Vancouver, Canada.

Vyazmensky, A., Stead, D., Elmo, D. and Moss, A. (2009a) Numerical analysis of block caving-induced instability in large open pit slopes: a finite element/discrete element approach, Rock Mechanics and Rock Engineering, DOI 10.1007/s00603-009-0035-3.

Vyazmensky, A., Elmo, D. and Stead, D. (2009b) Role of rock mass fabric and faulting in the development of block caving induced subsidence, Rock Mechanics and Rock Engineering, DOI 10.1007/s00603-009-0069-6.

Yan, M. (2008) Numerical modelling of brittle fracture and step-path failure: from laboratory to rock slope scale, PhD thesis, Simon Fraser University, Vancouver, Canada.

Yu, J. (1999) A contact interaction framework for numerical simulation of multi-body problems and aspects of damage and fracture for brittle materials, PhD thesis, University of Wales, Swansea, UK.